NeuroImage 114 (2015) 386–397

Contents lists available at ScienceDirect

NeuroImage

journal homepage: www.elsevier.com/locate/ynimg

# cTBS delivered to the left somatosensory cortex changes its functional connectivity during rest

Nikola Valchev [a,*], Branislava Ćurčić-Blake [a], Remco J. Renken [a], Alessio Avenanti [b], Christian Keysers [a,c], Valeria Gazzola [a,c,1], Natasha M. Maurits [a,d,**,1]

[a] University of Groningen, University Medical Center Groningen, Neuroimaging Center, Groningen, The Netherlands
[b] Department of Psychology and Center for Studies and Research in Cognitive Neuroscience, Cesena Campus, University of Bologna, Italy
[c] Netherlands Institute for Neuroscience, Royal Netherlands Academy of Arts and Sciences, Amsterdam, The Netherlands
[d] University of Groningen, University Medical Center Groningen, Department of Neurology, Groningen, The Netherlands

ARTICLE INFO

*Article history:*
Received 14 December 2014
Accepted 6 April 2015
Available online 13 April 2015

*Keywords:*
Primary somatosensory cortex
Connectivity
Resting-state
cTBS

ABSTRACT

The primary somatosensory cortex (SI) plays a critical role in somatosensation as well as in action performance and social cognition. Although the SI has been a major target of experimental and clinical research using non-invasive transcranial magnetic stimulation (TMS), to date information on the effect of TMS over the SI on its resting-state functional connectivity is very scant. Here, we explored whether continuous theta burst stimulation (cTBS), a repetitive TMS protocol, administered over the SI can change the functional connectivity of the brain at rest, as measured using resting-state functional magnetic resonance imaging (rs-fMRI). In a randomized order on two different days we administered active TMS or sham TMS over the left SI. TMS was delivered off-line before scanning by means of cTBS. The target area was selected previously and individually for each subject as the part of the SI activated both when the participant executes and observes actions. Three analytical approaches, both theory driven (partial correlations and seed based whole brain regression) and more data driven (Independent Component Analysis), indicated a reduction in functional connectivity between the stimulated part of the SI and several brain regions functionally associated with the SI including the dorsal premotor cortex, the cerebellum, basal ganglia, and anterior cingulate cortex. These findings highlight the impact of cTBS delivered over the SI on its functional connectivity at rest. Our data may have implications for experimental and therapeutic applications of cTBS over the SI.



## Introduction

Resting-state functional magnetic resonance imaging (rs-fMRI) is becoming the most popular method for studying functional connectivity in the brain, and has led to a surge of evidence that many neurological and psychiatric disorders present with abnormal functional connectivity. Transcranial magnetic stimulation (TMS) is the most frequently used method to experimentally change brain activity in healthy volunteers. A clinically relevant but relatively under-investigated question now becomes, whether functional brain connectivity, as measured using rs-fMRI, can be changed experimentally using TMS (see Fox et al., 2012) through an approach sometimes called "perturb-and-measure" or "condition-and-map" (Avenanti et al., 2007, 2013; Paus, 2005; Siebner et al., 2009). Only a few studies so far have investigated whether rs-fMRI changes after application of TMS, and most of these studies have used traditional repetitive TMS (Eldaief et al., 2011; Rahnev et al., 2013; van der Werf et al., 2010; Vercammen et al., 2010). In the last decade, a TMS protocol called continuous theta-burst stimulation (cTBS) has become increasingly popular for its capability to lead to long lasting changes of brain activity after only a few seconds of TMS application (Bertini et al., 2010; Conte et al., 2012; Franca et al., 2006; Huang et al., 2005). The standard cTBS protocol involves short bursts of high-frequency stimulation (50 Hz) repeated at the theta frequency (5 Hz) continuously for 40 s and it is based on the physiological pattern of neural firing found in the hippocampus of animals (Huang et al., 2009a,b; Kandel and Spencer, 1961). When applied to the motor cortex cTBS generally induces a transient reduction of cortical excitability (Huang et al., 2005, 2009a,b). Administration to other cortical areas also results in behavioural effects consistent with transient suppression of cortical excitability (Bertini et al., 2010; Conte et al., 2012; Franca et al., 2006; Rai et al., 2012). However, the nature of cTBS (and other TMS protocols) impact on neural processing is still intensely debated (Harris et al., 2008; Siebner et al., 2009; Silvanto and Pascual-Leone, 2012).

Although rs-fMRI may offer important insights into the mechanisms of action of cTBS by measuring its effect on functional connectivity of

* Correspondence to: N. Valchev, Neuroimaging Center, University Medical Center Groningen, A. Deusinglaan 2, 9713AW Groningen, The Netherlands.
** Correspondence to: N. Maurits, University Medical Center Groningen, Department of Neurology, AB51, PO Box 30001, 9700 RB Groningen, The Netherlands.
*E-mail addresses:* nikola.valtchev@gmail.com (N. Valchev), n.m.maurits@umcg.nl (N.M. Maurits).
[1] Contributed equally to the role of the last (senior) author.

http://dx.doi.org/10.1016/j.neuroimage.2015.04.017
1053-8119/

large-scale neural networks, to date only a few studies have combined cTBS and rs-fMRI. Moreover, their results are conflicting. In a first study, cTBS was applied over the occipital cortex, and the functional connectivity at rest was found to be reduced between V1, V2 and V3 (Rahnev et al., 2013), in line with the notion of a disruptive effect of cTBS when applied over the motor cortex (Huang et al., 2005). However, it should be noted that only 4 participants were recruited in that study and thus it is fundamental to test whether similar disruption of functional connectivity would also occur after cTBS over other brain regions, and whether the effect generalizes to a larger pool of participants. In a second study, Gratton et al. (2013) tested a larger sample of subjects and found increased connectivity in fronto-parietal and cingulo-opercular networks after cTBS over frontal sites (Gratton et al., 2013). However, these authors focused on brain activity acquired >20 min after the end of cTBS which may reflect the acute impact of frontal TMS in remote brain regions via neural interconnection but also the indirect influence of slower compensatory mechanisms (Avenanti et al., 2013; Lomber, 1999; Ruff et al., 2009). More recently, Mastropasqua et al. (2014) administered cTBS over the right dorsolateral prefrontal cortex in a sample of 18 participants and tested changes in brain areas functionally connected to the target region. In this case, data acquisition started approximately 5 min after the end of cTBS (Mastropasqua and Koch, personal communication). A reduction in the connectivity between the target region and the ipsilateral posterior parietal cortex was found. No similar changes were found in another group of subjects in which sham cTBS was administered.

The aim of this study was thus to further explore whether cTBS application would lead to changes of resting-state functional connectivity as measured with rs-fMRI. In particular, we aimed to use a counterbalanced cross-over design in which resting-state functional connectivity is measured after sham or active cTBS to ensure that unspecific psychological effects of believing to receive cTBS treatment would be subtracted out of a comparison. With this aim in mind, we decided to target a region of the primary somatosensory cortex (SI) involved during both the execution and observation of hand actions. The SI plays a fundamental role in somatosensation and action control. The SI has been a frequent target of previous TMS work and there is now an increasing interest for the possible therapeutic applications of non-invasive facilitation or downregulation of SI activity in a variety of conditions including chronic pain, focal dystonia, stroke and Parkinson's disease (Azañón and Haggard, 2009; Song et al., 2011a; Staines and Bolton, 2013). However, to date, little is known about the acute impact of non-invasive modulation of the SI on its resting-state functional connectivity.

At the core of healthy motor skills lie years of execution of motor actions, and these functions require tight and reciprocal interactions between motor structures and somatosensory regions processing the re-afferent somatosensory signals (e.g. Cui et al., 2014), providing a relatively well understood system of brain regions the connectivity of which can be explored as a function of cTBS over the SI. In addition, this system is not only recruited while performing actions: it has been shown that many of the brain regions involved in action execution are also active while viewing the actions of others (Caspers et al., 2010; Rizzolatti and Sinigaglia, 2010). In humans (for a review see Caspers et al., 2010), the system of brain areas activated both when subjects observe, and execute actions, which has been designated 'shared circuits' (Gazzola and Keysers, 2009), includes the traditional parieto-frontal mirror network, composed of the ventral premotor cortex (vPM), and the anterior part of the inferior parietal lobule (in particular, area PF), that are the homologues of the brain regions in which mirror neurons have been found most often in the monkey (Casile, 2013), as well as the dorsal premotor cortex (dPM) and SI (Caspers et al., 2010).

Because these brain regions interact both during motor execution and during action observation, we expect that they form a powerful test-bed for exploring whether cTBS on one of the nodes of this interconnected system would lead to changes in functional connectivity with the other regions (vPM, dPM or IPL). Here we therefore applied cTBS over the region of the SI active during both action observation and execution, and explored whether cTBS changed functional connectivity, as measured using rs-fMRI, in particular in the remaining nodes of the shared circuits (vPM, dPM or IPL).

However, since the SI is activated in a "mirror like" fashion in a variety of tasks (see Keysers et al., 2010 for a review) that go beyond action execution and observation, we also explored changes of functional connectivity following cTBS over the SI in the entire brain and inside the network of areas activated by both action observation and execution. Based on the results obtained by Rahnev et al. (2013) and Mastropasqua et al. (2014) and taking into account the methodological aspects of the study by Gratton et al. (2013) we expected that cTBS over the SI would decrease its functional connectivity with interconnected brain areas.

## Methods

### *Experimental procedures*

The experiment was divided into three sessions distributed over three days. The data reported in this experiment was collected together with the data reported in Valchev, Gazzola, Avenanti and Keysers (in preparation). Both reports use the action observation and execution data recorded on the first experimental day (localizer) to define the shared circuits and identify the target point for TMS, but while Valchev et al. (in preparation) focuses on the action observation data, here we focus on the resting-state sequence collected on the second and third days.

The data collected on the first day consisted of a high resolution anatomical scan which was immediately prepared for neuronavigation. Observation and execution runs followed the anatomical scan (see supplementary materials for more task details). Right after scanning, the individual resting motor threshold (rMT) was determined (see Transcranial magnetic stimulation section) and the corresponding optimal scalp position (OSP) was saved using neuronavigation software (Brain Innovation, Maastricht, The Netherlands) for further use.

From the participant's point of view the second and third experimental sessions were identical. However, the difference between the two days was that (in a randomized fashion) active or sham cTBS was delivered. We refer to the stimulation as active and sham to denote that the pulse sequence is the same, but the sham coil used to deliver sham cTBS produces no effective stimulation. Nine subjects received active cTBS on the second day and eight on the third day. Each day started with the identification of the target point for TMS, which was checked for consistency at each experimental session (see Target point selection and neuronavigation section). After marking the target point with a pen on a cap placed over the participants' head, subjects were taken to the MRI preparation room and positioned comfortably in the MRI bed. With the help of a wooden device placed behind their back, participants were able to stay half seated. In this way TMS could be delivered in the scanner bed. Stimulation was delivered after 5 min of rest during which participants were required to remain as relaxed as possible (see Transcranial magnetic stimulation section). Stimulation was delivered in the preparation room using the mark on the cap instead of online neuronavigation, because executing neuronavigation in the pre-scanner room would have required to evaluate the rMT there as well, which would have blocked the facilities for other use and experiments. Now, only TMS was applied in the pre-scanner room which was necessary to transport the participant as fast as possible into the scanner. The cap used was an electroencephalography (EEG) cap (without electrodes) with chin-strap, because these caps are designed not to move, and hence ensure that the neuronavigation marker does not move relative to the head while transporting the participant. After the stimulation (sham or active cTBS), the wooden device was removed carefully, repositioning the participant to a supine position. The bed with the participant was then transported to the scanner and about 5 min (mean 5.2 min, standard deviation = 0.4) after the end of TMS the scanning sequence was initiated. Scanning included (in this order)

an observation (~8 min duration) and resting-state scan (~12 min duration). Thus, the RS sequence acquisition started approximately 13 min after cTBS, well within the temporal window of the cTBS effect.

### Participants

A total of 24 participants took part in the study of which 18 completed all three sessions. One of these 18 subjects was excluded because there was no clear activation in the SI during the localizer. The final data set analysed here was thus composed of 17 subjects (6 female, age 18–25 years, mean 20.9 years, all right handed (Oldfield, 1971)). Of the 6 participants who did not complete all three sessions of the experiment, two had excessive resting motor threshold (>64% of maximum stimulator output),[2] two decided by themselves to quit after the second session, and two reported light headaches after the second session (involving sham cTBS stimulation for both of them) and were advised to discontinue participation. All subjects had normal or corrected-to-normal visual acuity in both eyes and were naïve to the purpose of the experiment. Full debriefing was provided only at the end of the third session. Participants gave written informed consent and received monetary compensation. Procedures were approved by the Medical Ethical Committee of the University Medical Center Groningen. None of the participants had any neurological, psychiatric or other medical problems or contraindications to TMS or fMRI.

### Transcranial magnetic stimulation

The cTBS protocol lasted 40 s and consisted of bursts of 3 TMS pulses delivered at 50 Hz, with bursts being repeated every 200 ms (at 5 Hz) for a total of 600 pulses (Bertini et al., 2010; Franca et al., 2006; Huang et al., 2005). Stimulation was administered with a 70 mm figure-eight stimulation coil connected to a Magstim Rapid2 (The Magstim Company, Carmarthenshire, Wales, UK). Sham cTBS was delivered with the same parameters but through a placebo coil (The Magstim Company, Carmarthenshire, Wales, UK) that produces a comparable noise and some scalp sensations for the subject but produces no effective stimulation. Subjects were all naïve to TMS and upon questioning after the experiment were unable to reliably differentiate between sham and active cTBS.

Previous studies have suggested that motor activity before, during or after the administration of active cTBS may alter its effect on cortical excitability (Huang et al., 2008; Iezzi et al., 2008, 2011; Todd et al., 2009). Therefore, participants rested for 5 min before stimulation and were asked to remain relaxed during and after stimulation. After cTBS, it took no more than 5 min to start scanning which permitted us to capture the effect of the stimulation when it reached its maximum level (Huang et al., 2005).

Stimulation was performed by placing the coil tangentially to the scalp over the individual's SI. Scalp position was localized by means of a neuronavigation system (see next paragraph). During neuronavigation and cTBS the coil was held approximately at a 45° angle away from the midline with the handle pointing backward and laterally, as various TMS protocols using this coil orientation were shown to be adept to affect SI processing (Ishikawa et al., 2007; Jacquet and Avenanti, 2015; Knecht et al., 2003; Oliveri et al., 1999; Ragert et al., 2008).

Pulse intensity was set at 80% rMT (mean 47.35% (SD 5.06)) of the maximum output (Nyffeler et al., 2006). This intensity is greater than that used in standard cTBS protocols, where 80% of active motor threshold (aMT) is typically used (Huang et al., 2005). Standard cTBS protocols are however optimized for suppressing excitability of the motor cortex and cTBS may produce smaller or shorter-lasting effects when applied over the SI relative to the motor cortex (Ishikawa et al., 2007; Rai et al., 2012; Staines and Bolton, 2013). The aforementioned rs-fMRI study of Gratton et al. (2013) did not observe changes in functional connectivity using standard cTBS intensity over the SI. Since stimulation intensity may play a role in the inhibitory effectiveness of cTBS (Goldsworthy et al., 2012), we decided to use an intensity of 80% rMT (which would correspond to about 90–95% of aMT) to increase the chances of observing an effect of cTBS on brain activity.

The rMT evaluation was performed by recording motor-evoked potentials (MEPs) induced by single-pulse TMS of the left motor cortex. MEPs were recorded from the right first dorsal interosseous (FDI) muscle using a Refa amplifier (TMSi, Enschede, The Netherlands). Pairs of silver/silver chloride surface electrodes were placed over the muscle belly (active electrode) and over the associated joint of the FDI muscle (reference electrode). A ground electrode was placed on the ventral surface of the right wrist. EMG signals were sampled at 5 kHz, band-pass filtered (20 Hz–1.0 kHz), digitized and displayed on a computer screen. The optimum scalp position (OSP) was chosen so as to produce maximum amplitude MEPs in the FDI muscle. The rMT was defined as the lowest level of stimulation able to induce MEPs of at least 50 μV with 50% probability (Rossini et al., 1994).

### Target point selection and neuronavigation

The area in the SI to be stimulated with cTBS was derived from the functional map obtained from the conjunction of the observation run and the execution run from the first (localizer) session for each individual subject using Brain Voyager (Brain Innovation, Maastricht, The Netherlands). First, a binary mask was created from the contrast (Action Execution)–(Execution Control), thresholded at $p_{unc} = 0.001$, and with a minimum cluster size of 10. The mask was then used to limit the contrast (Action Observation)–(Observation Control), thus selecting only voxels which were activated by both tasks. The threshold for the observation contrast was first set to $p_{unc} = 0.001$, min cluster size of 10 and then if needed, made more stringent to better identify the peak of activation in the SI (for the MNI coordinates of the target point for each participant see Fig. 2.1 and Table 2.1). Each individual subject map was overlaid on the anatomical 3D reconstruction of the individual grey–white matter boundary for use during online neuronavigation. We navigated to the target point by keeping the orientation of the coil at 45° from midline. We identified the projection of the SI on the scalp and then marked coil's position and orientation on the EEG cap. Mean Talairach coordinates for the activation target point were $-43 \pm 5.52$, $-31 \pm 5.98$, and $54 \pm 5.49$ (MNI: −43 −35 57 corresponds to the left postcentral gyrus, as defined in the Anatomy toolbox (Eickhoff et al., 2005, 2006, 2007)).

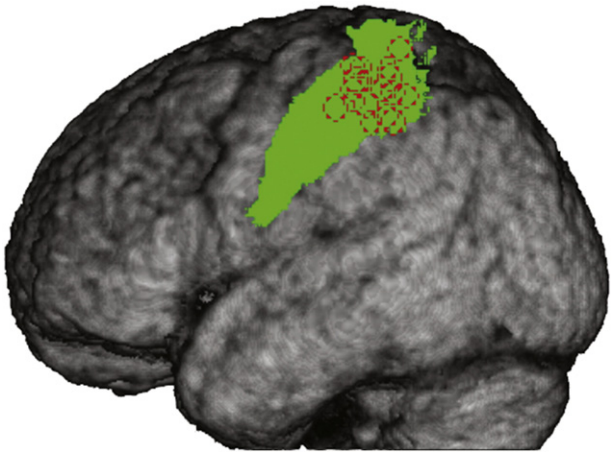

**Fig. 2.1.** Average grey matter segment from all 17 participants with areas BA1 and BA2 indicated in green and individual TMS target points as dotted red circles.

[2] This limitation is due to the technical characteristics of the TMS machine used in this experiment. The frequency of the cTBS stimulation (50 Hz) requires the capacitors of the machine to recharge at a rapid rate, which is not possible for stimulations at intensities of more than 51% (corresponding to 80% of the rMT of 64%).

**Table 2.1**
TAL and individually transformed MNI coordinates of the target point for each participant.

| Participant | TAL coordinates | Transformed MNI coordinates |
|---|---|---|
| 1 | −47 −28 51 | −47 −32 54 |
| 2 | −53 −26 51 | −54 −29 54 |
| 3 | −45 −24 60 | −45 −28 64 |
| 4 | −48 −33 45 | −48 −36 47 |
| 5 | −36 −39 65 | −36 −44 68 |
| 6 | −41 −25 54 | −41 −29 57 |
| 7 | −52 −22 48 | −53 −25 51 |
| 8 | −42 −28 55 | −42 −32 58 |
| 9 | −36 −36 57 | −36 −40 60 |
| 10 | −37 −36 53 | −37 −40 56 |
| 12 | −44 −26 56 | −44 −30 59 |
| 13 | −34 −38 46 | −34 −41 48 |
| 14 | −38 −36 47 | −38 −39 49 |
| 15 | −39 −35 60 | −39 −39 63 |
| 16 | −43 −42 53 | −43 −46 55 |
| 17 | −43 −28 59 | −43 −32 63 |
| 18 | −45 −33 53 | −45 −37 56 |

*Data acquisition and preprocessing*

Imaging was performed with a Philips Intera 3T with a synergy SENSE eight channel head coil and maximum gradient strength of 30 mT/m. The resting-state sequence employed standard single shot EPI with TE = 35 ms, TA = 1.95 s, TR = 2 s. For each volume, 37 AC–PC aligned axial slices of 3.5 mm thickness, without slice gap and a 3.5 × 3.5 mm in plane resolution were acquired to cover the entire brain using interleaved slice acquisition. A T1-weighted structural scan was acquired with TR = 7.657 ms, TE = 3.54 ms, flip angle = 8°, 1 × 1 × 1 mm voxel size. The images were preprocessed in SPM8 (http://www.fil.ion.ucl.ac.uk/spm/). We applied slice time correction to the EPI volumes from the resting-state run and realigned them to the mean image from the three observation task runs to bring all images to the same space. The T1 grey matter segment was co-registered to the mean resting-state EPI, and used to determine normalization parameters that were subsequently applied to all resting-state EPIs (2 × 2 × 2 mm). All data was then spatially smoothed using an 8 mm FWHM kernel. The functional images were further band-pass filtered from 0.01 Hz to 0.08 Hz using the Resting State fMRI Data Analysis toolbox (Song et al., 2011a,b) to focus on the frequency band shown to have the best signal-to-noise ratio when it comes to resting-state functional connectivity analyses.

*Confounds matrix Z*

In addition, we extracted a number of confounds to be used in multiple data-analysis approaches. For each subject and resting-state session, we extracted the time course of (i) the signal averaged over the whole brain, (ii) over the white matter and (iii) over the CSF signal. The average white matter and CSF signals were computed using the probability maps included in SPM8. By applying a threshold of 95% for the white matter and 75% for the CSF, we created binary maps and used those to extract the corresponding average signals (see e.g., Geerligs et al., 2012; Van Dijk et al., 2010). In addition, we included the 6 motion parameters and their first derivatives. These 15 variables are jointly referred to as the confounds matrix Z.

*Connectivity analysis methods*

We applied three analytical methods to the preprocessed data set to determine whether active cTBS over the SI modifies the functional connectivity at rest: partial correlations, whole brain regression and Independent Component Analysis. Throughout this manuscript, we will then use the term connectivity as short-hand for functional connectivity in the sense of synchronization of BOLD activity across regions. Exploring all three methods was motivated by the fact that there are two publications using a similar rs-fMRI and TMS combination and that no prior knowledge exists on the effect of cTBS over the SI on its functional connectivity during rest. Furthermore, the same combination of analytical approaches has been applied to RS data before by Doria et al. (2010). We performed a partial correlation analysis to evaluate if active cTBS delivered over the SI changed the connectivity in the shared circuits network. To evaluate if active cTBS changed the functional connectivity between the TMS targeted region and *any* other region in the brain we performed a seed based whole brain regression analysis. This analysis provides a voxel-wise localization of any change in connectivity in the shared circuits as should also be detected by the partial correlation analysis, as well as the localization of changes in connectivity elsewhere in the brain. The third analysis method applied to the data was spatial Independent Component Analysis (sICA) which was chosen as a data driven method which does not require the definition of a particular region of interest or seed.

*ROI definition and data extraction*

For each subject, a sphere with a diameter of 1 cm was built around the MNI coordinates of the target point using Marsbar (Brett et al., 2002). Subsequently, the sphere was intersected with the anatomical region of interest (ROI) consisting of BA1 and BA2 (as defined in the Anatomy toolbox in SPM8 (Eickhoff et al., 2005, 2006, 2007)), and with the corresponding the subject's grey matter segment to obtain the target ROI in the SI. We restricted the target ROI to BA1 and BA2 because they represent the integration area of the primary somatosensory cortex, receiving input from ipsilateral BA3a and BA3b, the contralateral BA2, and projecting connections to these areas (Jones, 1986; Shanks et al., 1985). This ROI is hereafter referred to as the target ROI in the SI.

To define the left parietal shared circuit node ROI, referred to as IPL (inferior parietal lobe), the group level shared circuits mask from the first experimental session (see supplementary materials) was intersected with an anatomical ROI corresponding to left area PF, as defined in the Anatomy toolbox in SPM (combining PF + PFcm + PFt + PFop + PFm). Left premotor ROIs were created by first combining the anatomical ROIs in the left BA6 and left BA44 (as defined in the Anatomy toolbox for SPM). Because these regions contain the ventral premotor (vPM), dorsal premotor (dPM) and the supplementary motor area (SMA), we first excluded all voxels between sagittal "x" coordinates −13 and 13 (SMA). The remaining region was split along the coronal "z" coordinate 48 into the vPM ($z < 48$) and dPM ($z \geq 48$) (Tomassini et al., 2007). Resulting ROIs were further limited by intersecting them with the shared circuits mask (see supplementary materials).

*Partial correlation analysis*

For each subject, and each ROI (target ROI in SI, IPL, vPM, dPM) we calculated the first eigenvector of the activations during the sham and active cTBS sessions, separately from the preprocessed data. Since the sign of the first eigenvector is arbitrary and can be positively or negatively correlated with the time series within the corresponding ROI, we controlled for a positive correlation between each eigenvector and the mean signal within the ROI from which it was extracted. Partial correlations were calculated between each pair of ROIs, controlling for the other pair of ROIs (or not) and confounds matrix Z (regressors of no interest). To compare partial correlations across sham and active cTBS, all correlations were first Fisher-Z transformed and these (now normally distributed as verified by Shapiro–Wilk tests, all $p > 0.05$) values were then compared using paired sample T-tests to evaluate whether cTBS over the target ROI in the SI induced a change in connectivity between any of the ROIs. Results of the six paired T-tests were corrected for multiple comparisons using Bonferroni correction.

*Whole brain regression analysis*

For each subject a design matrix for the first level SPM analysis was created. We included as a regressor of interest the first eigenvector from

**Table 3.1**
Mean partial correlations and standard deviations for each connection between ROIs as derived from the sham and active cTBS sessions, and T statistics and (uncorrected) p-values resulting from the paired T-tests. In the left 3 columns, the other ROIs are included, and in the right 3 columns, they are not included as nuisance variables in the partial correlations.

| Connection | Other ROIs as covariates | | | Other ROIs not included as covariates | | |
|---|---|---|---|---|---|---|
| | Sham cTBS | Active cTBS | Paired T-test | Sham cTBS | Active cTBS | Paired T-test |
| | Mean (SD) | Mean (SD) | | Mean (SD) | Mean (SD) | |
| SI–IPL | 0.25 (0.19) | 0.28 (0.24) | $T_{(16)} = -0.72$; $p = 0.48$ | 0.30(0.34) | 0.33(0.26) | $p = 0.64$ |
| SI–vPM | 0.28 (0.3) | 0.27 (0.24) | $T_{(16)} = 0.04$; $p = 0.97$ | 0.41 (0.36) | 0.41 (0.19) | $p = 0.95$ |
| SI–dPM | 0.5 (0.25) | 0.29 (0.32) | $T_{(16)} = 3.26$; $p = 0.005$ | 0.51 (0.25) | 0.33 (0.36) | $p = 0.007$ |
| IPL–vPM | 0.22 (0.23) | 0.26 (0.3) | $T_{(16)} = -0.56$; $p = 0.58$ | 0.33 (0.34) | 0.32 (0.36) | $p = 0.88$ |
| IPL–dPM | 0.12 (0.23) | 0.09 (0.27) | $T_{(16)} = 0.38$; $p = 0.71$ | −0.01 (0.25) | −0.002 (0.28) | $p = 0.89$ |
| vPM–dPM | 0.02 (0.17) | −0.06 (0.23) | $T_{(16)} = 1.15$; $p = 0.27$ | 0.12 (0.16) | −0.2 (0.25) | $p = 0.13$ |

the target ROI in the SI (extracted from the preprocessed data) and as regressor of no interest, to remove sources of regionally nonspecific variance, the confounds matrix Z. The parameter estimates associated with the first eigenvector regressor represent the voxelwise functional connectivity with the targeted region. Contrast images were then taken to the second level of analysis.

*Spatial Independent Component Analysis*

Spatial Independent Component Analysis (sICA) was performed on the preprocessed, temporally detrended and band-pass filtered images (Calhoun et al., 2009; Cardoso, 2003). GIFT v. 1.3 (Calhoun et al., 2001) as implemented in MatLab 7.5 was used to perform the analysis. The toolbox first applies sICA to the concatenated preprocessed data and then computes the session and subject specific components and time courses using the GICA3 algorithm (Calhoun et al., 2001; Schmithorst and Holland, 2004). The analysis we performed contained three stages: 1) data reduction, 2) calculation of the spatial independent components, and 3) back reconstruction. At the first stage, a principle component analysis was used to reduce the dimensionality of individual subject data. Then the Infomax algorithm (Bell and Sejnowski, 1995) was applied to estimate the spatial independent sources. We asked the algorithm to calculate a set of 10 Independent Components (ICs) based on the size of the shared circuits mask and on the existing literature on resting state sICA analysis (Van Den Heuvel and Hulshoff, 2010). Yeo et al. (2011) have already shown that using a clustering approach, consistent networks can be identified in a 7 networks solution. Since one of our questions was whether active cTBS induced any change in the connectivity between the targeted area in the SI and the rest of the shared circuits network, which is a relatively large network, we identified a smaller number of components which results in the identification of spatially larger ICs. In addition, a larger number of components would likely make it more difficult to detect a possible effect of cTBS stimulation since the algorithm could separate the induced changes in brain activity into different components. Not knowing the extent of the brain area(s) that will show the change of connectivity induced by TMS, we aimed to estimate a sufficiently high number of meaningful independent components while still identifying large networks so that the effects of the stimulation would be identifiable within the same component(s). Ten ICs also permit the identification of the main networks reported in the literature, as eight resting state networks have been consistently reported (Van Den Heuvel and Hulshoff, 2010): somato-motor, primary visual, extrastriate visual, insular-temporal/ACC, left parietal–frontal, right parietal-frontal, default mode and frontal networks. In the final stage, through back reconstruction, the individual subject and session image maps and time courses (one per IC) were computed. The value within each voxel represents the degree of correlation of its fMRI signal with the time course of the component.

From the 10 original ICs we selected the ones with the highest spatial correlation with the shared circuits mask. Only these components were used to investigate the effect of TMS over the SI. Statistics were obtained by applying a permutation test and randomly permuting the labels (sham cTBS and active cTBS, within subject) 10,000 times to obtain a null distribution. We then derived pseudo p-values for each voxel and comparison, based on a two-tailed approach and the position of the true data within the null-distribution. In order to correct for the multiple comparisons problem both voxel-wise and test-wise, the p-maps were thresholded using FDR correction (voxelwise and testwise).

## Results

*Partial correlation analysis*

Partial correlations were calculated between each pair of ROIs from the shared circuits network (target ROI in SI, IPL, vPM, dPM). Paired sample T-tests showed changes in the connectivity after active cTBS only between the target ROI in the SI and the dPM ROI ($T_{(16)} = 3.26$; $p = 0.005$; Bonferroni correction for applying six T-tests implied that results are significant when $p \leq 0.008$ (See Table 3.1, left)). Specifically, the SI and dPM were characterized by a positive partial correlation under sham cTBS, and this functional connectivity was reduced by active cTBS. The same was true if the partial correlations only controlled for the confounds matrix Z but not for the activity of the other ROIs (Table 3.1, right). We repeated the analysis using mean time courses within the ROI instead of the first eigen-timecourse, and found similar results, with only SI–dPM significantly changing functional connectivity under the influence of active cTBS.

*Whole brain regression analysis*

The first eigenvector of the time course in the target ROI in the SI from the sham and active cTBS sessions was used as regressor for each subject in the first level design matrix. Evaluating the contrast (sham cTBS)–(active cTBS) at the second level ($T_{(16)} \geq 3.69$; $p_{(uncor)} \leq 0.001$; min cluster size 10) showed that functional connectivity decreased due to active cTBS between the target ROI in the SI and a cluster in left BA6 (18 voxels), which is also part of the shared circuits network (see Fig. 3.1 and Table 3.2). In this cluster parameter estimates decreased under the influence of cTBS, from a peak parameter estimate (MNI: −22 −12 56) of 2.14 (sham cTBS) to 1.22 (active cTBS), confirming the effect found using partial correlations in the dPM ROI. Another cluster that survived this threshold was in the white matter (10 voxels). None of the clusters survived FDR correction. At a lower threshold of $T_{(16)} \geq 2.92$; $p_{(uncor)} \leq 0.005$; min cluster size of 20, both clusters identified previously grew in size; the one in the left BA6 increased to 207 voxels, the one in the white matter to 60, and one more cluster in the contralateral BA6 survived (88 voxels). The opposite contrast (active cTBS)–(sham cTBS) also showed no clusters surviving FDR correction. At a threshold of $p_{(uncor)} \leq 0.001$ ($T_{(16)} \geq 3.69$; min cluster size 10) several clusters appeared in the left middle temporal gyrus, precuneus, inferior parietal lobule and middle frontal gyrus and the right middle occipital gyrus. When lowering the threshold to $p_{(uncor)} \leq 0.005$ ($T_{(16)} \geq 2.92$; min cluster size 20[3]) several additional clusters scattered throughout the white and grey matter appear.

[3] The larger cluster size of 20 is used to take the more lenient significance level (0.005 instead of 0.001) into account.

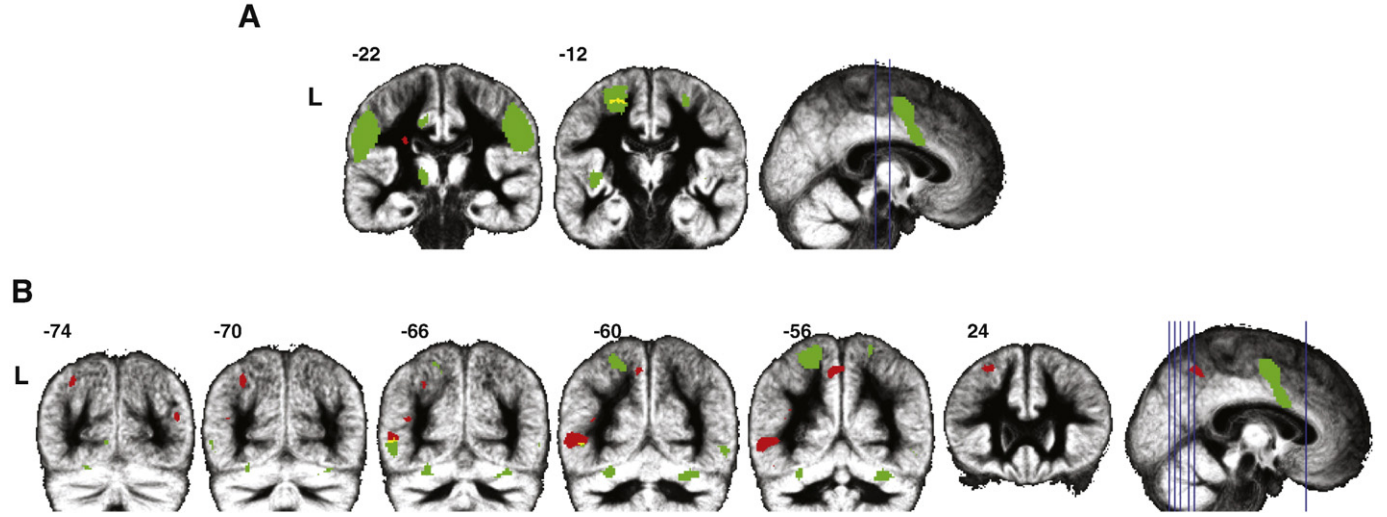


**Fig. 3.1.** Group results from the whole brain regression analysis. A: Reductions of functional connectivity with SI (contrast (sham cTBS)–(active cTBS)) are shown in red, the shared circuits mask in green, and the overlap in yellow. B: Increases in functional connectivity with the SI (contrast (active cTBS)–(sham cTBS)) are shown in red, the shared circuits mask in green. All contrasts are shown at $T_{(16)} \geq 3.69$; $p_{(uncor)} \leq 0.001$; min cluster size 10.

To assess local effects of cTBS, we further compared the variance of the fMRI signal in the target ROI in the SI after sham cTBS and after active cTBS. We extracted the time series for each voxel in each individual target ROI in the SI and calculated the mean standard deviation per subject across voxels in the target ROI per experimental session. We then compared the values from the sham and the active cTBS sessions using standard T-tests and found no significant difference between them ($t(16) = 1.19$; $p = 0.24$). This suggests that the reported changes in SI connectivity are not associated with local reductions of variance of fMRI signal.

*Spatial Independent Component Analysis*

To check whether active cTBS over the SI induced a change in the ICs related to the shared circuits network we sorted the mean spatial maps from the sham cTBS and active cTBS sessions separately, according to their spatial correlation with the shared circuits mask (see Fig. 3.2). We selected the networks with the highest spatial correlation with the shared circuits mask and ordered them according to the strength of the correlation. Four networks were selected, named hereafter A, B, C and D (spatial maps resulting from the sham cTBS session) and A′, B′, C′ and D′ (spatial maps resulting from the active cTBS session). Networks A from the sham cTBS session and A′ from the active cTBS session showed the highest spatial correlation with the mask ($r = 0.39$ for A and $r = 0.38$ for A′), followed by components B and B′ ($r = 0.11$ for both B and B′), components C and C′ ($r = 0.1$ for both C and C′) and components D and D′ ($r = 0.09$ for D and $r = 0.08$ for D′). Examining the mean values across voxels and participants in the target ROI in the SI for each component map – which provides an estimate of the mean correlation between the voxel time courses and the component time course – showed that the networks vary with regard to how strongly the cTBS target point belongs to that particular network (is 'included'; Table 3.3): networks A & A′, which tightly match the dorsal SI/MI network reported in the literature moderately include the SI target point (mean value $r_A = 0.181$, $r_{A'} = 0.147$). Networks B & B′, resembling the network commonly associated to the central executive/attentional networks but also including anterior parts of the precentral gyrus, include the target point moderately ($r_B = 0.103$, $r_{B'} = 115$), followed by networks D (0.094) and D′ (0.095). Finally, networks C (−0.001) and C′ (0.004), include the ventral parts of the SI, and not the target point, but incorporate many of the brain regions receiving information from the SI to process sensory and emotional aspects of somatosensation, including SII, the insula and the anterior cingulate. We chose to compare the spatial maps of these four components because they represent the highest spatial correlation with the shared circuits mask and with the SI in particular (all other components show a correlation close to zero) and their spatial maps include not only regions of the mask but they represent networks that relate to the motor, sensory or emotional functions of the SI (see Fig. 3.2).

Results of the permutation test showed significant differences between the spatial maps from the sham and active cTBS sessions in each of the four selected components. In the pair of spatial maps of components A and A′ differences were localized in the right precuneus, putamen and amygdala, and the left superior frontal gyrus, caudate nucleus and cerebellum. For the pair of spatial maps of components B and B′ the left cuneus and precentral gyrus and right precentral gyrus, supramarginal gyrus, anterior cingulate cortex and middle frontal gyrus were identified. Spatial maps of components C and C′ showed a significant difference in the right middle orbital gyrus and the spatial maps of components D and D′ differed significantly in the right superior medial gyrus. Of these clusters the left superior frontal gyrus (BA6) (when comparing spatial maps A and A′), and the right supramarginal gyrus (OP1)

**Table 3.2**
Group results for the whole brain regression analysis, contrasts (sham cTBS)–(active cTBS) and (active cTBS)–(sham cTBS) at $T_{(16)} \geq 3.69$; $p_{(uncor)} \leq 0.001$; min cluster size of 10, with and without masking with the shared circuits map, cluster size k in voxels and for the local maxima within each cluster: corresponding T value, MNI coordinates (x, y, z) in mm, hemisphere (R: right, L: left), anatomical localization and, cytoarchitectonic localization when available (as given by the Anatomy toolbox).

| k | T | x | y | z | Hem | Anatomical description | Cytoarchitectonic description |
|---|---|---|---|---|---|---|---|
| *(Sham cTBS)–(active cTBS) not masked* | | | | | | | |
| 18 | 4.15 | −22 | −12 | 56 | L | Superior frontal gyrus | BA 6 |
| 10 | 4.36 | −26 | −22 | 26 | L | White matter | |
| *(Sham cTBS)–(active cTBS) masked with shared circuits* | | | | | | | |
| 17 | 4.16 | −22 | −12 | 56 | L | Superior frontal gyrus | BA6 |
| *(Active cTBS)–(sham cTBS) not masked* | | | | | | | |
| 180 | 5.28 | −52 | −60 | 2 | L | Middle temporal gyrus | |
| 82 | 5.19 | −6 | −56 | 50 | L | Precuneus | SPL |
| 49 | 4.69 | −30 | −70 | 42 | L | Inferior parietal lobule | SPL |
| 31 | 4.36 | −40 | −66 | 16 | L | Middle temporal gyrus | |
| 15 | 4.04 | −26 | 24 | 50 | L | Middle frontal gyrus | |
| 10 | 4.12 | 44 | −74 | 16 | R | Middle occipital gyrus | IPC |
| *(Active cTBS)–(sham cTBS) masked with shared circuits* | | | | | | | |
| 22 | 5.11 | −50 | −62 | 0 | L | Middle temporal gyrus | hOC5 |

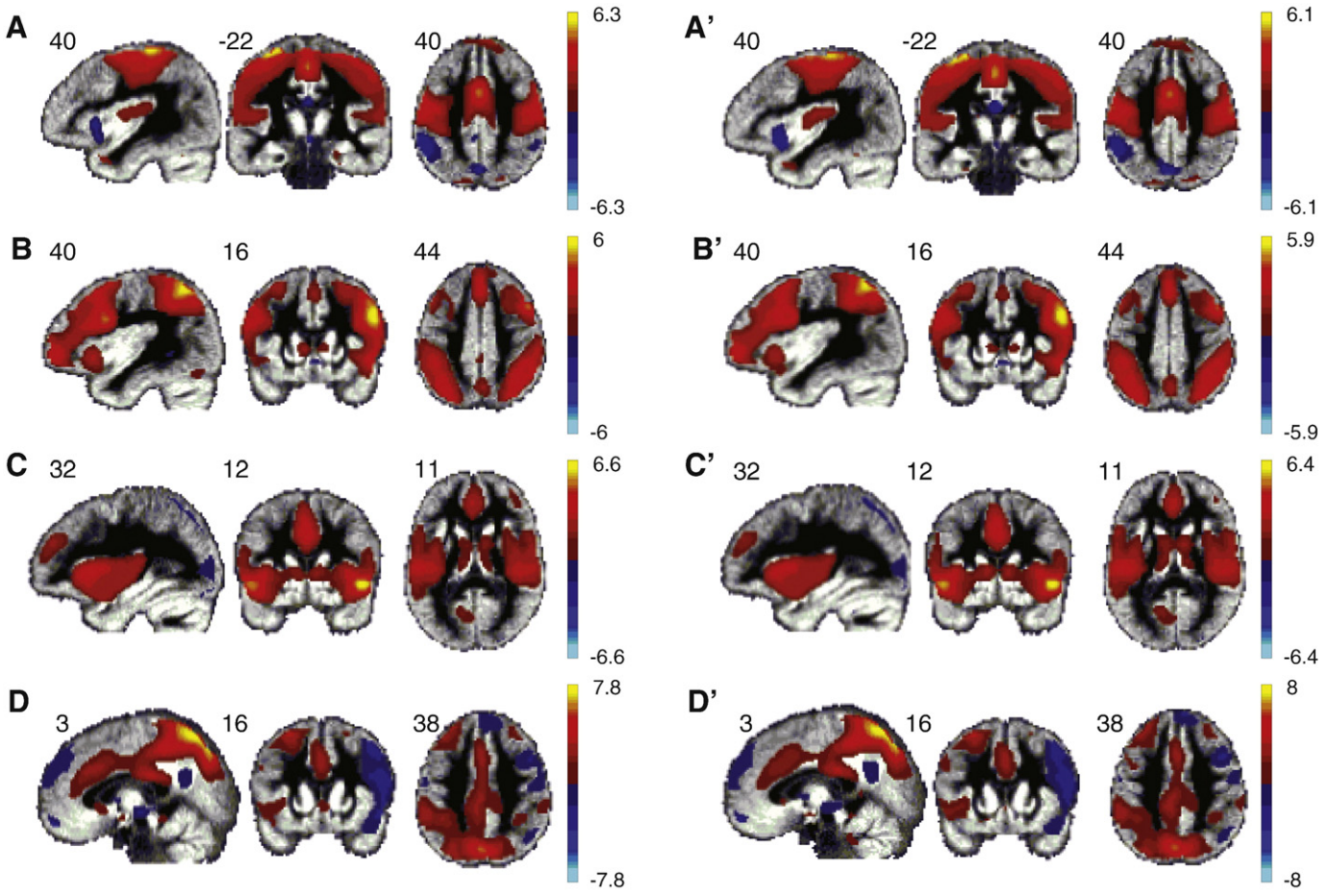


**Fig. 3.2.** Spatial maps of the components resulting from the sICA that are spatially correlated with the shared circuits mask. Components A, B, C and D were derived from the sham cTBS resting-state data and A′, B′, C′ and D′ were derived from the active cTBS resting-state data. Values in each spatial map represent the normalized correlation of each voxel with the estimated time course of the corresponding component thresholded at $-1 \leq z \leq 1$.

and left precentral gyrus (BA6) (when comparing spatial maps B and B′), were located inside the shared circuits map (see Fig. 3.3). Although the permutation test we used is two-tailed and unsigned, we also considered the direction of differences in the clusters identified by this procedure, and the degree to which each component spatial map includes the SI target ROI (Table 3.3). With only one exception in the

**Table 3.3**
Results of the permutation test comparing the spatial maps of all four components from the sham and active cTBS sessions, selected on the basis of their spatial correlation with the shared circuits mask; cluster size k in voxels and for the centre of mass for each cluster: MNI coordinates (x, y, z) in mm, hemisphere (R: right, L: left), anatomical localization, cytoarchitectonic localization when available (as given by the Anatomy toolbox), and an indication of how many voxels from the cluster are included in the shared circuits mask. Results FDR-corrected for both voxel-wise and test-wise multiple comparisons. The second column reflects the direction of the difference, based on a post-hoc T-test within the cluster. For each component, the mean value (over voxels and participants) in the target ROI in SI is indicated.

| k | Direction | x | y | z | Hem | Anatomical description | Cytoarchitectonic description | In SC mask Y/N |
|---|---|---|---|---|---|---|---|---|
| *A–A′ (mean value in target ROI in SI: A = 0.181; A′ = 0.147)* | | | | | | | | |
| 58 | A > A′ | 14 | −66 | 38 | R | Precuneus | | N |
| 27 | A > A′ | −24 | −8 | 52 | L | Superior frontal gyrus | Area 6 | Y (34 voxels) |
| 26 | A > A′ | −14 | 12 | 6 | L | Caudate nucleus | | N |
| 22 | A > A′ | −34 | −76 | −20 | L | Cerebellum | hOC4v (V4) | N |
| 21 | A > A′ | 26 | −76 | −20 | R | Cerebellum | VI | N |
| 14 | A > A′ | 30 | 6 | −4 | R | Putamen | | N |
| 10 | A > A′ | 26 | 2 | −16 | R | Amygdala | Amyg (SF) | N |
| *B–B′ (mean value in target ROI in SI: A = 0.103; A′ = 0.115)* | | | | | | | | |
| 78 | B > B′ | −2 | −66 | 22 | L | Cuneus | | N |
| 22 | B > B′ | 48 | −10 | 52 | R | Precentral gyrus | Area 6 | N |
| 22 | B > B′ | 62 | −18 | 18 | R | Parietal operculum | OP1 | Y (2 voxels) |
| 17 | B < B′ | −26 | −14 | 58 | L | Precentral gyrus | Area 6 | Y (18 voxels) |
| 14 | B > B′ | 2 | 30 | −4 | R | Anterior cingulate cortex | | N |
| 13 | B > B′ | 30 | 48 | 22 | R | Middle frontal gyrus | | N |
| *C–C′ (mean value in target ROI in SI: A = −0.001; A′ = 0.004)* | | | | | | | | |
| 12 | C > C′ | 44 | 52 | −8 | R | Middle orbital gyrus | | N |
| *D–D′ (mean value in target ROI in SI: A = 0.094; A′ = 0.095)* | | | | | | | | |
| 36 | D > D′ | 4 | 68 | 8 | R | Superior medial gyrus | | N |

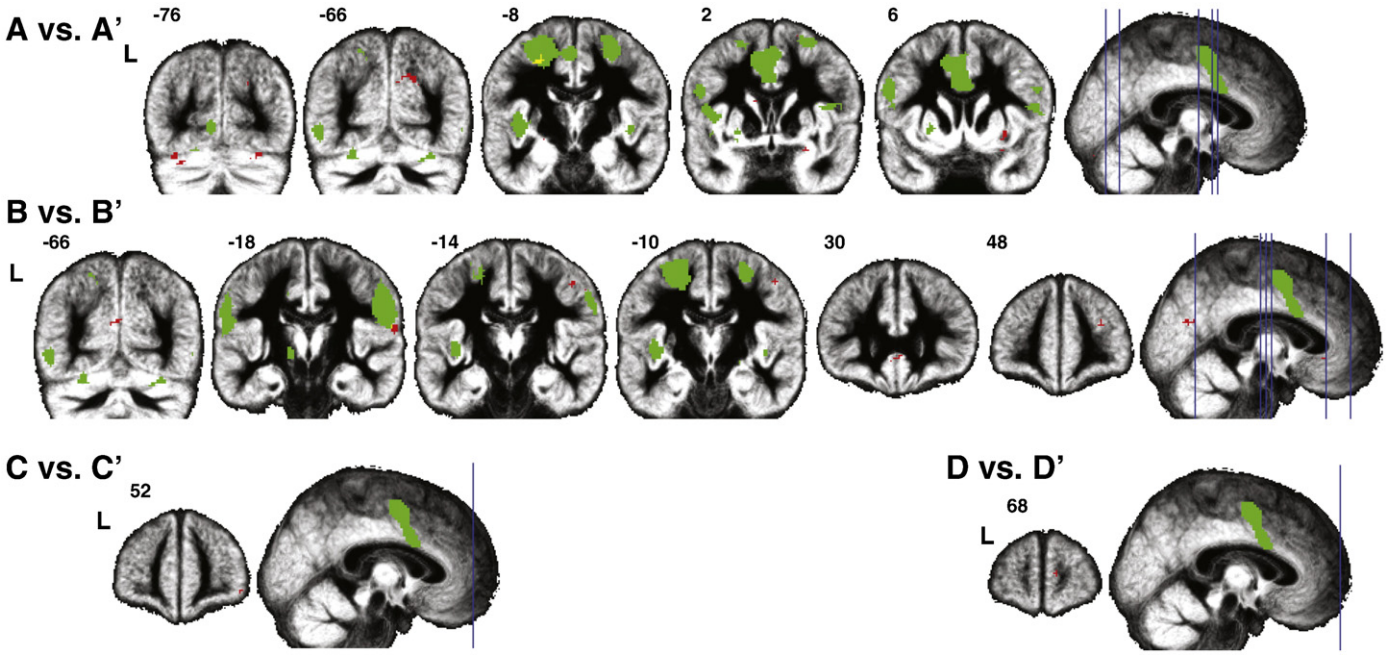


**Fig. 3.3.** Results from the permutation test comparing the spatial maps of all four components. In green the shared circuits mask and in red (or yellow whenever there is an overlap) the clusters where voxels show significant differences between the spatial maps of the sham and active cTBS sessions. Results are FDR-corrected for both voxel-wise and test-wise multiple comparisons.

left precentral gyrus, active cTBS resulted in a reduced integration of the clusters at hand in the component, i.e. active cTBS reduced the functional connectivity between these clusters and the network in which they are normally integrated.

## Discussion

In this study we explored whether cTBS over the SI can alter functional connectivity as measured during rest using an offline combination of cTBS and fMRI. We compared the spontaneous activations in the brain during rest after subjects received active cTBS or sham cTBS over the part of the left SI activated by both action execution and action observation. The main finding of our study was that cTBS over the SI did alter functional connectivity as measured with rs-fMRI. In particular, the partial correlation and seed based whole brain regression analysis showed that the functional connectivity between the stimulated region in the SI and an ipsilateral left dPM cluster, falling within the shared circuits, was reduced by active cTBS. The sICA confirmed this reduction of functional connectivity following active cTBS when we considered the networks which are spatially correlated with the shared circuits. In particular there are 2 sub-regions in the left dPM which appear to be synchronized differentially with two different networks (and therefore with SI) depending on the type of stimulation. One more anterior region (Table 3.3, contrast A > A′) shows higher synchronization with network A (thus after sham), while this connectivity is reduced after cTBS. The second more posterior sub-region (Table 3.3, contrast B < B′) shows higher synchronization with network B′ (thus after cTBS), than after sham stimulation. Outside the shared circuits, sICA showed that cTBS over the SI reduced the degree to which a number of brain regions participate in the four ICs we explored, including in particular a number of brain regions known to be strongly associated with the SI during the planning, execution and observation of motor actions (basal ganglia, cerebellum, BA6 (Rizzolatti et al., 1996)), the processing of tactile stimuli and the observation of touch in others (SII in the parietal operculum, (Keysers et al., 2004)) and the experience and observation of nociceptive stimuli (anterior cingulate, amygdala, (Duerden and Albanese, 2013; Lamm et al., 2011)). Importantly, this network includes regions known to have direct or indirect connections with the region of the SI we have targeted (Jones, 1986; Pandya and Vignolo, 1971; Shanks et al., 1985; Wise et al., 1997). We must stress that not having a functional measurement of the effectiveness of our stimulation limits our conclusions. For this reason we cannot show how changes in connectivity at rest caused by cTBS stimulation over the SI affect behaviour or information processing during active task performance. However, we make no claim on the functional role of the connections we have evidenced but we show that cTBS over the SI affects its connectivity. This is, to our knowledge, the first study which finds an effect of cTBS over the SI as measured with resting-state fMRI. We put in evidence not only the connectivity of the SI during rest but also the potential use of TMS as a therapeutic tool which can affect resting-state connectivity.

Here we found that cTBS over the SI reduces the functional connectivity of brain regions with the target region. In the partial correlation approach, we found a significant reduction but no significant increase in the connectivity between the dPM and SI. The sICA approach also evidenced reductions of functional connectivity, as revealed by lower correlations between identified clusters and the characteristic time-course of the examined components following active cTBS compared with sham. The only increase in correlation was found in the dPM relative to component B′. The whole brain seed-based approach was the only method that did not yield significant results when corrected for multiple comparisons, and should thus be interpreted more tentatively. This approach confirmed, not surprisingly given its methodological similarity to the partial correlation approach, that the dPM reduced its functional connectivity with the SI ($p < 0.001$ but $q_{fdr} > 0.05$), but also revealed a number of increases of functional connectivity. The fact that many of the latter fell within regions of the occipital and temporal lobe not anatomically connected to the SI, and that their false discovery rate is above 0.05 suggests that these increases may be due to chance.

Since we have no independent measure of the effectiveness of the cTBS in our participants (e.g. by measuring somatosensory evoked potentials, SEPs) we cannot be sure that cTBS was effective in all participants. Large variability in the effects of cTBS has been demonstrated with MEPs induced by motor cortex stimulation (see Hamada et al., 2012; Martin et al., 2006; Ridding and Ziemann, 2010). In that sense our results should be taken as an indication that at the group level,

cTBS weakens the functional connectivity of the SI during rest. How strong a reduction of connectivity is associated with a given neurophysiological local effect on the SI as measured using SEPs or the behavioural effects associated with this change of connectivity remain for future studies to explore. However, we find interesting that previous studies have documented that cTBS over the SI reduces those SEP components thought to be generated in somatosensory and premotor networks (i.e. the P22/N30 and P25/N33 components; (Ishikawa et al., 2007)). Future studies might directly test whether such SEP modulation reflects a reduction in the functional connectivity between the dPM and SI as we detected in our study.

Our findings of a reduction of resting-state functional connectivity may appear in contrast with those of Gratton et al. (2013) who did not see changes after cTBS over the SI. However, in that study authors focused on brain activity acquired >20 min after cTBS and used a standard cTBS intensity (80% of aMT). Since standard cTBS protocols over the SI show relatively short-lasting behavioural and electrophysiological effects (Ishikawa et al., 2007; Rai et al., 2012; Staines and Bolton, 2013) and greater stimulation intensity may increase suppressive efficiency of cTBS (Goldsworthy et al., 2012), in the present study we tried to maximize the chance of observing cTBS modulation by using greater intensity (80% of rMT) and starting our acquisition some minutes earlier (about 13 min) relative to the study of Gratton et al. (2013).

That the overall effect of cTBS seems to be a reduction in functional connectivity, matches the findings in four participants that cTBS over the occipital lobe (administered at an intensity of 80% of phosphene threshold, which is even higher to that used in our study, cf Deblieck et al., 2008) leads to a reduction in the functional connectivity between V1, V2 and V3 as measured during rest (Rahnev et al., 2013). In this study, resting-state data acquisition started after a short rotating-wedge retinotopy session, about 13 min after the end of cTBS (Rahnev et al., 2013), which is similar to our acquisition timing. A reduction in functional connectivity after cTBS was also found by Mastropasqua et al. (2014) who started the acquisition of the resting-state session 5 min after the end of active cTBS and used a standard cTBS intensity (80% of active motor threshold). Taken together, our study and the three previous cTBS rs-fMRI studies, may suggest that the effect of cTBS mainly consists in a reduction of resting-state functional connectivity, but stimulation intensity and timing of data acquisition may influence the direction of such effect. Further studies are needed to systematically investigate the effect of the targeted brain region, cTBS intensity and timing of acquisition on rs-fMRI. On the other hand, although tentative, our conclusion that cTBS protocols, thought to reduce cortical excitability, are capable of decreasing resting state functional connectivity is complemented by very recent findings showing that intermittent TBS (iTBS), which should increase cortical excitability (Huang et al., 2005), also increases resting state functional connectivity (Brusa et al., 2014; Nettekoven et al., 2014).

That the relationship between activation in the SI and dPM that was found to be disrupted according to all three methods used in this study is interesting in the context of what we know about the anatomy of these connections. In the monkey brain the dPM and the posterior part of the SI (areas 1 and 2) have strong *indirect* connections that are mediated by regions of the superior parietal lobe including the medial bank of the intraparietal sulcus, but direct connections between the dPM and SI have not been consistently reported (Ghosh and Gattera, 1995; Tanné-Gariépy et al., 2002). One of the merits of rs-fMRI, as opposed to diffusion weighted imaging, is its capacity to probe such indirect functional connectivity, but it is noteworthy that active cTBS over the SI did not show its most consistent effects in regions having direct connectivity with the SI (such as the posterior parietal lobe, PPL, including area PF investigated in the partial correlation analysis). Instead, the most consistent effect was in a premotor region that is consistently co-activated with the SI during action observation and execution (see for example Caspers et al., 2010), but that only has indirect anatomical connectivity. At present, we can only speculate about the physiological mechanisms behind such a remote effect. If cTBS was blocking directly the output of the SI, one would expect that regions directly receiving output from the SI, namely the PPL, would show the strongest reduction of functional connectivity with the SI — this was not consistently observed in our study. If cTBS was instead, to alter the millisecond scale synchronization of spiking across different output neurons in the SI, i.e. perturbing what has been considered binding in the gamma range (Ainsworth et al., 2012), while leaving fluctuations in the overall spike-rate in the second time-scale unaltered, one might expect the observed pattern of results: PPL neurons directly receiving input from the SI might still follow the changes in spike-rate in the second time-scale, and hence show normal functional connectivity in the frequency range measured with rs-fMRI. However, layer 5 pyramidal neurons that would compute the output to be sent to the next processing stage (dPM) have been shown to be exquisitely sensitive to the millisecond timing of convergent inputs (Ainsworth et al., 2012), and altering this timing in the SI would then reduce the impact of SI information on the output neurons in PPL regions. Accordingly, the dPM that receives input from these PPL output neurons would then become less influenced by SI activity, explaining the distal drop of rs-fMRI functional connectivity we observed. While entirely speculative, evidence that cTBS over the SI can indeed alter binding and fine-grained temporal coding stems from studies showing altered temporal order judgement in humans following cTBS application over the SI (Lee et al., 2013). Also, there is EEG evidence that cTBS can alter neural synchronization of various bands including the gamma band (Schindler et al., 2008) with some differential modulations for higher relative to lower frequency oscillators (Noh et al., 2012; Vernet et al., 2013). In addition animal evidence shows that cTBS alters the function of interneurons that regulate the pyramidal output neurons, and could thus provide the neural mechanism for such a perturbation of synchronicity (Benali et al., 2011; Funke and Benali, 2011; Hamada et al., 2012).

Some methodological aspects of our study require discussion. First, the target point for our stimulation was defined on the basis of the task performed on the first experimental day. An alternative approach would be to consider the task results (i.e. the activation in SI during action observation and execution) in combination with the baseline functional connectivity of the SI as input for the target point. However, given the size of the target area (BA1 and BA2 combined) and the area of influence of the TMS on the cortex, results would most likely be very similar.

Second, incidentally, non-specific changes in functional connectivity might occur between the sham cTBS and active cTBS sessions if they are on two different days. Notably, these changes would be random, and would average out after many repetitions. In order to make certain that these changes do not affect our results we randomized the order of sham cTBS and active cTBS between participants. Our design included only two counterbalanced post-cTBS scans (active vs sham cTBS) performed on two separate days, in contrast to the other previous cTBS-rs-fMRI studies that used a pre–post test design for each cTBS session (Gratton et al., 2013; Mastropasqua et al., 2014; Rahnev et al., 2013). While this latter design may be optimal to detect intra-session changes due to cTBS, nonetheless, our approach was sensitive enough to detect changes in resting-state functional connectivity between sham and active post-cTBS sessions.

Third, one critical aspect of comparing sham and active stimulations in cross-over designs is that these two stimulation conditions differ in terms of scalp sensations. Comparing cTBS to another form of active TBS such as intermediate TBS (imTBS) we might have been able to contrast the effects of cTBS over the SI with an active stimulation condition that is very similar to cTBS in terms of scalp sensations but, contrary to cTBS, is supposed not to affect cortical excitability (Huang et al., 2005). However, this assumption is mainly based on studies assessing the effect of TBS with motor-evoked potentials induced by the stimulation of the motor cortex (Huang et al., 2005, 2011). In contrast with such

an assumption, in a previous study it was found that active cTBS and imTBS over the SI similarly altered the amplitude of somatosensory-evoked potentials (SEPs), whereas sham TBS did not (Poreisz et al., 2008). Thus, because of our focus on S1, in designing our experiment we considered sham cTBS to be a better control condition to investigate the effects of active cTBS. However, it should be noted that the use of the Magstim sham coil does not exclude the possibility that our participants distinguished active from sham stimulation. The Magstim sham coil produces noise similar to active stimulation but the tactile sensations associated with active TMS stimulation are not induced. On the other hand, it is likely that differences in peripheral sensations had very little or no influence on our data because: 1) cTBS lasted only 40 s, occurred offline, at a low intensity and on a region of the scalp that is not particularly sensitive (e.g. in comparison to frontal or temporal areas); 2) our rsfMRI acquisition started 13 min after the end of stimulation. Furthermore, we performed two cTBS sessions on different days which were immediately followed by fMRI scans to keep participants as naïve as possible; and 3) no subjects reported any tactile sensations in their right hand which might have been used to distinguish the active from the sham cTBS protocols. Thus it is unlikely that the reduction of functional connectivity in sensorimotor areas we observed here could result from participants' knowledge about the cTBS condition.

Fourth, we also need to consider the possibility that passive viewing of human actions clips performed by our subjects immediately before the resting-state run might have influenced the resting-state networks reported in this paper. It has been shown that tasks that are performed before resting-state data are collected might have an effect on both the default mode network and task-positive networks (Albert et al., 2009; Barnes et al., 2009; Evers et al., 2012; Jolles et al., 2013). While we cannot exclude the possibility of an interaction between our action observation task and the subsequently collected resting-state data, we can expect that the effects of our 10 min of passive exposure to action movies prior to the resting-state run are small. In fact some studies have shown that a high cognitive demand task (Barnes et al., 2009) or a motor learning task (Albert et al., 2009), influences the resting-state network's activity. However, different studies show different effects of the performed task on resting-state functional connectivity. Evers et al. (2012) found a reduction in functional connectivity in task-related resting-state networks after a task of 1.5 h. Jolles et al. (2013) found an increase in functional connectivity related to a task performed on regular sessions during six weeks. Therefore, the relatively short duration of our action observation task and its low cognitive demands (i.e. passive viewing) would suggest little or no influence on resting-state functional connectivity, although further direct evidence is needed to directly assess the possible effect of action observation on rsfMRI. In our experiment resting-state data was collected always after the observation task, regardless whether the stimulation delivered before scanning was active or sham cTBS. Considering the possibility that resting-state networks might be affected by the previously performed action observation task, we could expect that both of our resting-state data sets (collected after active and sham cTBS) are equally affected by our short passive viewing task. We aimed to minimize the variability produced by previous states by having always the same order of experimental tasks. For this reason in our study we draw conclusions on the effects of cTBS on the functional connectivity of the SI during rest only after 8 min of action observation task.

In conclusion we have shown that cTBS over a brain region can reduce the functional connectivity of that brain region with the rest of the brain as measured using rs-fMRI. This type of “inhibitory” TMS protocol over the part of the left somatosensory cortex activated by both action observation and execution led to a reduction of the connectivity between this region and part of the ipsilateral dPM during rest. In addition to the cluster in the dPM, stimulating the SI with cTBS revealed reduced functional connectivity with other brain regions known to interact with the SI during action observation and execution (the basal ganglia, and cerebellum) as well as during the observation and experience of neutral (SII) and nociceptive (amygdala, anterior cingulate cortex) somatosensory stimuli. These results provide novel insights into the cortical effects of cTBS and might have implications for experimental and clinical applications of SI TBS including the modulation of tactile, proprioceptive and nociceptive processing (see for example Antal et al., 2008; Ishikawa et al., 2007; Ploner et al., 2002; Poreisz et al., 2008; Ragert et al., 2008) and the potential treatment of pathological states like chronic pain, focal dystonia, stroke and Parkinson's disease which may benefit from targeting the SI (Song et al., 2011a; Staines and Bolton, 2013).

## Author contributions

Conceived and designed the experiment: VG, CK and AA. Performed the experiment: NV, VG. Analysed the data: NV, BCB, NM, CK, helped by RR. Wrote the paper: NV, BCB, NM, CK, VG, AA. RR commented on the data analysis and the manuscript.

## Acknowledgments

The work was supported by a grant from the Portuguese Foundation for Science and Technology (FCT) co-funded by the Program for Human Potential and the European Union to NV (SFRH/BD/47576/2008), a N.W.O. VENI grant (451-09-006 MaGW) to VG, a Marie Curie Excellence Grant (MEXT-CT-2005-023253) from the European Commission and an ERC grant (312511) to CK and a Ministero della Salute (GR-2010-2319335), a Cogito Foundation (R-117/13) and MIUR grant (RBFR12F0BD) to AA. B.C-B and N.M.M. received UMCG grant (No.689901). B.C-B was also supported by the ERC grant awarded to A. Aleman. We would like to thank Inge Zijdewind and Peter Albronda for the help and equipment to record EMG, Simone Sprenger for helping with the neuronavigation, Idil Kokal and Luca Nanetti for helping during data collection, and Anita Kuipers, Judith Streurman, Marc Thioux and Luca Nanetti for the help with scanning. We thank Linda Geerligs for her suggestions regarding the preprocessing steps, and Bauke de Jong for a fruitful discussion during data analysis, and Rajat Thomas and Leonardo Cerliani for helpful discussions on the formal relationship between the three analyses used and the resting-state networks identified.

## Appendix A. Supplementary data

Supplementary data to this article can be found online at http://dx.doi.org/10.1016/j.neuroimage.2015.04.017.

## References

Ainsworth, M., Lee, S., Cunningham, M.O., Traub, R.D., Kopell, N.J., Whittington, M.A., 2012. Rates and rhythms: a synergistic view of frequency and temporal coding in neuronal networks. Neuron 75 (4), 572–583.

Albert, N.B., Robertson, E.M., Miall, R.C., 2009. The resting human brain and motor learning. Curr. Biol. 19 (12), 1023.

Antal, A., Brepohl, N., Poreisz, C., Boros, K., Csifcsak, G., Paulus, W., 2008. Transcranial direct current stimulation over somatosensory cortex decreases experimentally induced acute pain perception. Clin. J. Pain 24 (1), 56–63.

Avenanti, A., Bolognini, N., Maravita, A., Aglioti, S.M., 2007. Somatic and motor components of action simulation. Curr. Biol. 17 (24), 2129–2135.

Avenanti, A., Annella, L., Candidi, M., Urgesi, C., Aglioti, S.M., 2013. Compensatory plasticity in the action observation network: virtual lesions of STS enhance anticipatory simulation of seen actions. Cereb. Cortex 23, 570–580.

Azañón, E., Haggard, P., 2009. Somatosensory processing and body representation. Cortex 45 (9), 1078–1084.

Barnes, A., Bullmore, E.T., Suckling, J., 2009. Endogenous human brain dynamics recover slowly following cognitive effort. PLoS One 4 (8), e6626.

Bell, A.J., Sejnowski, T.J., 1995. An information-maximization approach to blind separation and blind deconvolution. Neural Comput. 7 (6), 1129–1159.

Benali, A., Trippe, J., Weiler, E., Mix, A., Petrasch-Parwez, E., Girzalsky, W., Eysel, U.T., Erdmann, R., Funke, K., 2011. Theta-burst transcranial magnetic stimulation alters cortical inhibition. J. Neurosci. Off. J. Soc. Neurosci. 31 (4), 1193–1203.

Bertini, C., Leo, F., Avenanti, A., Ladavas, E., 2010. Independent mechanisms for ventriloquism and multisensory integration as revealed by theta-burst stimulation. Eur. J. Neurosci. 31 (10), 1791–1799.

Brett, M., Anton, J.L., Valabregue, R., Poline, J.B., 2002. Region of interest analysis using an SPM toolbox [abstract] presented at the 8th International Conference on Functional Mapping of the Human Brain, June 2–6, 2002, Sendai, Japan. NeuroImage 16 (2).
Brusa, L., Ponzo, V., Mastropasqua, C., Picazio, S., Bonnì, S., Di Lorenzo, F., Iani, C., Stefani, A., Stanzione, P., Caltagirone, C., 2014. Theta burst stimulation modulates cerebellar-cortical connectivity in patients with progressive supranuclear palsy. Brain Stimul. 7 (1), 29–35.
Calhoun, V., Adali, T., Pearlson, G., Pekar, J., 2001. A method for making group inferences from functional MRI data using independent component analysis. Hum. Brain Mapp. 14 (3), 140–151.
Calhoun, V.D., Liu, J., Adalı, T., 2009. A review of group ICA for fMRI data and ICA for joint inference of imaging, genetic, and ERP data. NeuroImage 45 (1), S163–S172.
Cardoso, J., 2003. Dependence, correlation and Gaussianity in independent component analysis. J. Mach. Learn. Res. 4, 1177–1203.
Casile, A., 2013. Mirror neurons (and beyond) in the macaque brain: an overview of 20 years of research. Neurosci. Lett. 540, 3–14.
Caspers, S., Zilles, K., Laird, A.R., Eickhoff, S.B., 2010. ALE meta-analysis of action observation and imitation in the human brain. NeuroImage 50 (3), 1148–1167.
Conte, A., Rocchi, L., Nardella, A., Dispenza, S., Scontrini, A., Khan, N., Berardelli, A., 2012. Theta-burst stimulation-induced plasticity over primary somatosensory cortex changes somatosensory temporal discrimination in healthy humans. PLoS One 7 (3), e32979.
Cui, F., Arnstein, D., Thomas, R.M., Maurits, N.M., Keysers, C., Gazzola, V., 2014. Functional magnetic resonance imaging connectivity analyses reveal efference-copy to primary somatosensory area, BA2. PLoS One 9 (1), e84367.
Deblieck, C., Thompson, B., Iacoboni, M., Wu, A.D., 2008. Correlation between motor and phosphene thresholds: a transcranial magnetic stimulation study. Hum. Brain Mapp. 29 (6), 662–670.
Doria, V., Beckmann, C.F., Arichi, T., Merchant, N., Groppo, M., Turkheimer, F.E., Counsell, S.J., Murgasova, M., Aljabar, P., Nunes, R.G., 2010. Emergence of resting state networks in the preterm human brain. Proc. Natl. Acad. Sci. 107 (46), 20015–20020.
Duerden, E.G., Albanese, M., 2013. Localization of pain-related brain activation: a meta-analysis of neuroimaging data. Hum. Brain Mapp. 34 (1), 109–149.
Eickhoff, S.B., Stephan, K.E., Mohlberg, H., Grefkes, C., Fink, G.R., Amunts, K., Zilles, K., 2005. A new SPM toolbox for combining probabilistic cytoarchitectonic maps and functional imaging data. NeuroImage 25 (4), 1325–1335.
Eickhoff, S.B., Heim, S., Zilles, K., Amunts, K., 2006. Testing anatomically specified hypotheses in functional imaging using cytoarchitectonic maps. NeuroImage 32 (2), 570–582.
Eickhoff, S.B., Paus, T., Caspers, S., Grosbras, M.H., Evans, A.C., Zilles, K., Amunts, K., 2007. Assignment of functional activations to probabilistic cytoarchitectonic areas revisited. NeuroImage 36 (3), 511–521.
Eldaief, M.C., Halko, M.A., Buckner, R.L., Pascual-Leone, A., 2011. Transcranial magnetic stimulation modulates the brain's intrinsic activity in a frequency-dependent manner. Proc. Natl. Acad. Sci. 108 (52), 21229–21234.
Evers, E.A., Klaassen, E.B., Rombouts, S.A., Backes, W.H., Jolles, J., 2012. The effects of sustained cognitive task performance on subsequent resting state functional connectivity in healthy young and middle-aged male schoolteachers. Brain Connect. 2 (2), 102–112.
Fox, M.D., Halko, M.A., Eldaief, M.C., Pascual-Leone, A., 2012. Measuring and manipulating brain connectivity with resting state functional connectivity magnetic resonance imaging (fcMRI) and transcranial magnetic stimulation (TMS). NeuroImage 62 (4), 2232–2243.
Franca, M., Koch, G., Mochizuki, H., Huang, Y.Z., Rothwell, J.C., 2006. Effects of theta burst stimulation protocols on phosphene threshold. Clin. Neurophysiol. 117 (8), 1808–1813.
Funke, K., Benali, A., 2011. Modulation of cortical inhibition by rTMS—findings obtained from animal models. J. Physiol. 589 (18), 4423–4435.
Gazzola, V., Keysers, C., 2009. The observation and execution of actions share motor and somatosensory voxels in all tested subjects: single-subject analyses of unsmoothed fMRI data. Cereb. Cortex 19 (6), 1239–1255.
Geerligs, L., Maurits, N.M., Renken, R.J., Lorist, M.M., 2012. Reduced specificity of functional connectivity in the aging brain during task performance. Hum. Brain Mapp. 35 (1), 319–330.
Ghosh, S., Gattera, R., 1995. A comparison of the ipsilateral cortical projections to the dorsal and ventral subdivisions of the macaque premotor cortex. Somatosens. Mot. Res. 12 (3-4), 359–378.
Goldsworthy, M.R., Pitcher, J.B., Ridding, M.C., 2012. A comparison of two different continuous theta burst stimulation paradigms applied to the human primary motor cortex. Clin. Neurophysiol. 123 (11), 2256–2263.
Gratton, C., Lee, T.G., Nomura, E.M., D'Esposito, M., 2013. The effect of theta-burst TMS on cognitive control networks measured with resting state fMRI. Front. Syst. Neurosci. 7.
Hamada, M., Murase, N., Hasan, A., Balaratnam, M., Rothwell, J.C., 2012. The role of interneuron networks in driving human motor cortical plasticity. Cereb. Cortex 23 (7), 1593–1605.
Harris, J.A., Clifford, C.W., Miniussi, C., 2008. The functional effect of transcranial magnetic stimulation: signal suppression or neural noise generation? J. Cogn. Neurosci. 20 (4), 734–740.
Huang, Y.Z., Edwards, M.J., Rounis, E., Bhatia, K.P., Rothwell, J.C., 2005. Theta burst stimulation of the human motor cortex. Neuron 45 (2), 201–206.
Huang, Y.Z., Rothwell, J.C., Edwards, M.J., Chen, R.S., 2008. Effect of physiological activity on an NMDA-dependent form of cortical plasticity in human. Cereb. Cortex (New York, N.Y.) 18 (3), 563–570.
Huang, Y., Sommer, M., Thickbroom, G., Hamada, M., Pascual-Leonne, A., Paulus, W., Classen, J., Peterchev, A.V., Zangen, A., Ugawa, Y., 2009a. Consensus: new methodologies for brain stimulation. Brain Stimul. 2 (1), 2–13.
Huang, Y.Z., Rothwell, J.C., Lu, C.S., Wang, J., Weng, Y.H., Lai, S.C., Chuang, W.L., Hung, J., Chen, R.S., 2009b. The effect of continuous theta burst stimulation over premotor cortex on circuits in primary motor cortex and spinal cord. Clin. Neurophysiol. 120 (4), 796–801.
Huang, Y.Z., Rothwell, J.C., Chen, R.S., Lu, C.S., Chuang, W.L., 2011. The theoretical model of theta burst form of repetitive transcranial magnetic stimulation. Clin. Neurophysiol. 122 (5), 1011–1018.
Iezzi, E., Conte, A., Suppa, A., Agostino, R., Dinapoli, L., Scontrini, A., Berardelli, A., 2008. Phasic voluntary movements reverse the aftereffects of subsequent theta-burst stimulation in humans. J. Neurophysiol. 100 (4), 2070–2076.
Iezzi, E., Suppa, A., Conte, A., Voti, P.L., Bologna, M., Berardelli, A., 2011. Short-term and long-term plasticity interaction in human primary motor cortex. Eur. J. Neurosci. 33 (10), 1908–1915.
Ishikawa, S., Matsunaga, K., Nakanishi, R., Kawahira, K., Murayama, N., Tsuji, S., Huang, Y.Z., Rothwell, J.C., 2007. Effect of theta burst stimulation over the human sensorimotor cortex on motor and somatosensory evoked potentials. Clin. Neurophysiol. 118 (5), 1033–1043.
Jacquet, P.O., Avenanti, A., 2015. Perturbing the action observation network during perception and categorization of actions' goals and grips: state-dependency and virtual lesion TMS effects. Cereb. Cortex 1–11.
Jolles, D.D., Van Buchem, M.A., Crone, E.A., Rombouts, S.A., 2013. Functional brain connectivity at rest changes after working memory training. Hum. Brain Mapp. 34 (2), 396–406.
Jones, E.G., 1986. Connectivity of the primate sensory-motor cortex. Anonymous Sensory-motor Areas and Aspects of Cortical Connectivity. Springer, pp. 113–183.
Kandel, E.R., Spencer, W.A., 1961. Electrophysiology of hippocampal neurons. II. After-potentials and repetitive firing. J. Neurophysiol. 24, 243–259.
Keysers, C., Wicker, B., Gazzola, V., Anton, J.L., Fogassi, L., Gallese, V., 2004. A touching sight: SII/PV activation during the observation and experience of touch. Neuron 42 (2), 335–346.
Keysers, C., Kaas, J.H., Gazzola, V., 2010. Somatosensation in social perception. Nat. Rev. Neurosci. 11 (6), 417–428.
Knecht, S., Ellger, T., Breitenstein, C., Ringelstein, E.B., Henningsen, H., 2003. Changing cortical excitability with low-frequency transcranial magnetic stimulation can induce sustained disruption of tactile perception. Biol. Psychiatry 53 (2), 175–179.
Lamm, C., Decety, J., Singer, T., 2011. Meta-analytic evidence for common and distinct neural networks associated with directly experienced pain and empathy for pain. NeuroImage 54 (3), 2492–2502.
Lee, K.G., Jacobs, M.F., Asmussen, M.J., Zapallow, C.M., Tommerdahl, M., Nelson, A.J., 2013. Continuous theta-burst stimulation modulates tactile synchronization. BMC Neurosci. 14 (1), 1–9.
Lomber, S.G., 1999. The advantages and limitations of permanent or reversible deactivation techniques in the assessment of neural function. J. Neurosci. Methods 86 (2), 109–117.
Martin, P., Gandevia, S., Taylor, J., 2006. Theta burst stimulation does not reliably depress all regions of the human motor cortex. Clin. Neurophysiol. 117 (12), 2684–2690.
Mastropasqua, C., Bozzali, M., Ponzo, V., Giulietti, G., Caltagirone, C., Cercignani, M., Koch, G., 2014. Network based statistical analysis detects changes induced by continuous theta-burst stimulation on brain activity at rest. Front. Psychol. 5.
Nettekoven, C., Volz, L.J., Kutscha, M., Pool, E., Rehme, A.K., Eickhoff, S.B., Fink, G.R., Grefkes, C., 2014. Dose-dependent effects of theta burst rTMS on cortical excitability and resting-state connectivity of the human motor system. J. Neurosci. 34 (20), 6849–6859.
Noh, N.A., Fuggetta, G., Manganotti, P., Fiaschi, A., 2012. Long lasting modulation of cortical oscillations after continuous theta burst transcranial magnetic stimulation. PLoS One 7 (4), e35080.
Nyffeler, T., Wurtz, P., Lüscher, H., Hess, C.W., Senn, W., Pflugshaupt, T., von Wartburg, R., Lüthi, M., Müri, R.M., 2006. Repetitive TMS over the human oculomotor cortex: comparison of 1-hz and theta burst stimulation. Neurosci. Lett. 409 (1), 57–60.
Oldfield, R.C., 1971. The assessment and analysis of handedness: the Edinburgh inventory. Neuropsychologia 9 (1), 97–113.
Oliveri, M., Rossini, P.M., Pasqualetti, P., Traversa, R., Cicinelli, P., Palmieri, M.G., Tomaiuolo, F., Caltagirone, C., 1999. Interhemispheric asymmetries in the perception of unimanual and bimanual cutaneous stimuli. A study using transcranial magnetic stimulation. Brain J. Neurol. 122, 1721–1729.
Pandya, D.N., Vignolo, L.A., 1971. Intra- and interhemispheric projections of the precentral, premotor and arcuate areas in the rhesus monkey. Brain Res. 26 (2), 217–233.
Paus, T., 2005. Inferring causality in brain images: a perturbation approach. Philos. Trans. R. Soc. Lond. B Biol. Sci. 360 (1457), 1109–1114.
Ploner, M., Gross, J., Timmermann, L., Schnitzler, A., 2002. Cortical representation of first and second pain sensation in humans. Proc. Natl. Acad. Sci. U. S. A. 99 (19), 12444–12448.
Poreisz, C., Antal, A., Boros, K., Brepohl, N., Csifcsák, G., Paulus, W., 2008. Attenuation of N2 amplitude of laser-evoked potentials by theta burst stimulation of primary somatosensory cortex. Exp. Brain Res. 185 (4), 611–621.
Ragert, P., Franzkowiak, S., Schwenkreis, P., Tegenthoff, M., Dinse, H.R., 2008. Improvement of tactile perception and enhancement of cortical excitability through intermittent theta burst rTMS over human primary somatosensory cortex. Exp. Brain Res. 184 (1), 1–11.
Rahnev, D., Kok, P., Munneke, M., Bahdo, L., de Lange, F.P., Lau, H., 2013. Continuous theta burst transcranial magnetic stimulation reduces resting state connectivity between visual areas. J. Neurophysiol. 110 (8), 1811–1821.
Rai, N., Premji, A., Tommerdahl, M., Nelson, A., 2012. Continuous theta-burst rTMS over primary somatosensory cortex modulates tactile perception on the hand. Clin. Neurophysiol. 123 (6), 1226–1233.

Ridding, M.C., Ziemann, U., 2010. Determinants of the induction of cortical plasticity by non-invasive brain stimulation in healthy subjects. J. Physiol. 588 (13), 2291–2304.
Rizzolatti, G., Sinigaglia, C., 2010. The functional role of the parieto-frontal mirror circuit: interpretations and misinterpretations. Nat. Rev. Neurosci. 11 (4), 264–274.
Rizzolatti, G., Fadiga, L., Matelli, M., Bettinardi, V., Paulesu, E., Perani, D., Fazio, F., 1996. Localization of grasp representations in humans by PET: 1. Observation versus execution. Exp. Brain Res. 111 (2), 246–252.
Rossini, P., Barker, A., Berardelli, A., Caramia, M., Caruso, G., Cracco, R., Dimitrijevic, M., Hallett, M., Katayama, Y., Lucking, C., 1994. Non-invasive electrical and magnetic stimulation of the brain, spinal cord and roots: Basic principles and procedures for routine clinical application. report of an IFCN committee. Electroencephalogr. Clin. Neurophysiol 91 (2), 79–92.
Ruff, C.C., Driver, J., Bestmann, S., 2009. Combining TMS and fMRI: from 'virtual lesions' to functional-network accounts of cognition. Cortex 45 (9), 1043–1049.
Schindler, K., Nyffeler, T., Wiest, R., Hauf, M., Mathis, J., Hess, C.W., Müri, R., 2008. Theta burst transcranial magnetic stimulation is associated with increased EEG synchronization in the stimulated relative to unstimulated cerebral hemisphere. Neurosci. Lett. 436 (1), 31–34.
Schmithorst, V.J., Holland, S.K., 2004. Comparison of three methods for generating group statistical inferences from independent component analysis of functional magnetic resonance imaging data. J. Magn. Reson. Imaging 19 (3), 365–368.
Shanks, M., Pearson, R., Powell, T., 1985. The callosal connexions of the primary somatic sensory cortex in the monkey. Brain Res. Rev. 9 (1), 43–65.
Siebner, H.R., Bergmann, T.O., Bestmann, S., Massimini, M., Johansen-Berg, H., Mochizuki, H., Bohning, D.E., Boorman, E.D., Groppa, S., Miniussi, C., 2009. Consensus paper: combining transcranial stimulation with neuroimaging. Brain Stimul. 2 (2), 58–80.
Silvanto, J., Pascual-Leone, A., 2012. Why the assessment of causality in brain–behavior relations requires brain stimulation. J. Cogn. Neurosci. 24 (4), 775–777.
Song, S., Sandrini, M., Cohen, L.G., 2011a. Modifying somatosensory processing with non-invasive brain stimulation. Restor. Neurol. Neurosci. 29 (6), 427–437.
Song, X.W., Dong, Z.Y., Long, X.Y., Li, S.F., Zuo, X.N., Zhu, C.Z., He, Y., Yan, C.G., Zang, Y.F., 2011b. REST: a toolkit for resting-state functional magnetic resonance imaging data processing. PLoS One 6 (9), 1–12.
Staines, W.R., Bolton, D.A., 2013. Transcranial magnetic stimulation techniques to study the somatosensory system: research applications. Handb. Clin. Neurol. 116, 671–679.
Tanné-Gariépy, J., Rouiller, E.M., Boussaoud, D., 2002. Parietal inputs to dorsal versus ventral premotor areas in the macaque monkey: evidence for largely segregated visuomotor pathways. Exp. Brain Res. 145 (1), 91–103.
Todd, G., Flavel, S.C., Ridding, M.C., 2009. Priming theta-burst repetitive transcranial magnetic stimulation with low- and high-frequency stimulation. Exp. Brain Res. 195 (2), 307–315.
Tomassini, V., Jbabdi, S., Klein, J.C., Behrens, T.E., Pozzilli, C., Matthews, P.M., Rushworth, M.F., Johansen-Berg, H., 2007. Diffusion-weighted imaging tractography-based parcellation of the human lateral premotor cortex identifies dorsal and ventral subregions with anatomical and functional specializations. J. Neurosci. 27 (38), 10259–10269.
Valchev, N., Gazzola, V., Avenanti, A., Keysers, C., 2015. Somatosensory contribution to action observation brain activity - a combined fMRI and cTBS study (in preparation).
Van Den Heuvel, M., Hulshoff, Pol H., 2010. Exploring the brain network: a review on resting-state fMRI functional connectivity. Eur. Neuropsychopharmacol. 20 (8), 519–534.
van der Werf, Y., Sanz-Arigita, E., Menning, S., van den Heuvel, O., 2010. Modulating spontaneous brain activity using repetitive transcranial magnetic stimulation. BMC Neurosci. 11 (1), 145.
Van Dijk, K.R.A., Hedden, T., Venkataraman, A., Evans, K.C., Lazar, S.W., Buckner, R.L., 2010. Intrinsic functional connectivity as a tool for human connectomics: theory, properties, and optimization. J. Neurophysiol. 103 (1), 297–321.
Vercammen, A., Knegtering, H., Liemburg, E.J., Boer, J.Ad., Aleman, A., 2010. Functional connectivity of the temporo-parietal region in schizophrenia: effects of rTMS treatment of auditory hallucinations. J. Psychiatr. Res. 44 (11), 725–731.
Vernet, M., Bashir, S., Yoo, W., Perez, J.M., Najib, U., Pascual-Leone, A., 2013. Insights on the neural basis of motor plasticity induced by theta burst stimulation from TMS–EEG. Eur. J. Neurosci. 37 (4), 598–606.
Wise, S.P., Boussaoud, D., Johnson, P.B., Caminiti, R., 1997. Premotor and parietal cortex: corticocortical connectivity and combinatorial computations 1. Annu. Rev. Neurosci. 20 (1), 25–42.
Yeo, B.T., Krienen, F.M., Sepulcre, J., Sabuncu, M.R., Lashkari, D., Hollinshead, M., Roffman, J.L., Smoller, J.W., Zollei, L., Polimeni, J.R., et al., 2011. The organization of the human cerebral cortex estimated by intrinsic functional connectivity. J. Neurophysiol. 106 (3), 1125–1165.